Mikrochim. Acta 132, 219–224 (2000)

Mikrochimica Acta

Mathematical Modelling of 3D Electron-Photon Transport in Microbeam Analysis

Jorge E. Fernández*, **Vincenzo G. Molinari,** and **Francesco Teodori**

National Institute of Physics of Matter (INFM) and Laboratory of Montecuccolino-DIENCA, University of Bologna, Via dei Colli,16 40136 Bologna, Italy

Abstract. In electron microbeam techniques, the particle beam is focused on the material to be analysed. When the electron beam enters the target, the electrons give rise to ionization processes producing secondary electrons and photons, the latter being used to characterize the material. As a consequence, a detailed description of the photon diffusion requires the solution of two coupled equations describing respectively electron and photon diffusion. The approach considering two transport equations, even if formally correct, is almost unaffordable because of the high mathematical complexity of the electron transport equation. In this article, an alternative approach is suggested which is based on the use of an approximate solution for the electron transport using the Fokker-Planck equation [5]. The resulting electron distribution, computed analytically as a solution of the above equation, is very similar to the ionization distribution and is used as the source term in the Boltzmann transport equation describing the photon diffusion in the material. The 3D photon transport equation for unpolarised photons with this source term is solved to obtain a detailed description of the photon fluorescence from a homogeneous slab.

Key words: Electron transport; Fokker-Planck equation; photon transport; photoelectric effect; photon angular distribution.

In electron microbeam techniques, photon production is stimulated by an electron beam focused on the target. The process of electron diffusion and slowing down is complicated. Energy losses occur through various kinds of inelastic interactions between the diffusing electrons and the target atoms. Most of the interactions involve the excitation of atomic electrons and gives rise to energy losses of few eV. Energy losses of several keV also occur, when an inner shell is ionized, but are relatively infrequent. An incident electron of 10 keV or more undergoes several interactions down to thermalisation, which is the reason why the continuous slowing down approximation, as introduced by Lewis and Spencer, is often used [1 – 4].

In this paper such approximation is removed and the Fokker-Planck equation is used. The analytical treatment is difficult without introducing some simplifying hypothesis consisting in disregarding one or another effect. Here the direction straggling has been neglected and energy dependence considered, because the ionization cross sections depend on energy. This simpler equation has been solved exactly, obtaining the depth distribution and the energy spectrum of the electrons. The ionization distribution has been also evaluated and has been used as the source term of a 3D photon transport equation for unpolarised photons. Such equation has been solved to obtain a detailed description of the photon fluorescence from a homogeneous slab with an inner diffuse source. The prevailing photoelectric effect has been considered for describing in first approximation the multiple scattering correction to source photons escaping towards the detector.

The Electron Distribution

Let us consider a perpendicular plane electron source hitting a target with speed v_0. By denoting with η the cosine of the angle between the direction of the

* To whom correspondence should be addressed

electron travel and the initial velocity vector $\vec{v}_0$, the Fokker-Planck equation for the distribution function is given by [5]

$$\eta v \frac{\partial}{\partial z} f(z,v,\eta) = \frac{\partial}{\partial v^2}\left[\frac{\beta}{v} f(z,v,\eta)\right] + \frac{\partial}{\partial v}\left[\frac{\alpha}{v^2} f(z,v,\eta)\right] + \frac{\gamma}{v^2}\frac{\partial}{\partial \eta}\left[(1-\eta^2)\frac{\partial}{\partial \eta} f(z,v,\eta)\right] + S(z,v,\eta) \quad (1)$$

There is no dependence on the azimuth because of the azimuthal isotropy of the Coulomb cross sections. α is the dynamical friction coefficient while γ and β are the coefficients of the diffusion velocity tensor. For Coulomb interactions they are expressed as follows:

$$\alpha = nM\Theta\left[1 - M\left(1 - \frac{1}{2}\ln\Lambda\right)\right];$$
$$\beta = nM^2\frac{\Theta}{2}\ln\Lambda;$$
$$\gamma = nM^2\frac{\Theta}{2}\left(1 - \frac{1}{2}\ln\Lambda\right);$$
$$\Theta = \frac{e^4 \ln\Delta}{4\pi\varepsilon_0^2 m'^2}; M = \frac{m'}{m_e} = \frac{1}{2};$$
$$\Delta = \frac{1}{\tan(\chi_0/2)}; \quad (2)$$

where m' is the reduced electron mass and χ_0 is the minimum deflection angle in the center of mass system.

During the slowing down, when $v \gg (3\,kT/m_t)^{1/2}$, due to the anisotropy of the Coulomb scattering the persistence of the velocity after a collision is enhanced. So we assume that during the slowing down the component of the velocity along v_0 is predominant ($\eta \approx 1$). The Fokker-Planck equation (1) becomes

$$v\frac{\partial}{\partial z} f(z,v) = \frac{\partial}{\partial v^2}\left[\frac{\beta}{v} f(z,v)\right] + \frac{\partial}{\partial v}\left[\frac{\alpha}{v^2} f(z,v)\right] + N_0\delta(z)\delta(v - v_0) \quad (3)$$

With the boundary condition

$$\lim_{z\to\infty} f(z,v) = 0 \quad (4)$$

the following solution has been found [5]

$$f(z,v) = \frac{4N_0}{v_0^2}\left(\frac{v}{v_0}\right)^{2(1-p)} \sum_{n=0}^{\infty} \frac{J_p(j_{p-1,n}((v/v_0))^2)}{J_p(j_{p-1,n})} \cdot \exp\left[-\frac{4j_{p-1,n}^2\beta}{v_0^4} z\right]. \quad (5)$$

In this equation $j_{p,n}$ is the n-th zero of the Bessel function of order p. The Bessel function order depends on the characteristics of the medium according to the relation

$$p = \frac{1 + \alpha/\beta}{4}. \quad (6)$$

Starting from equation (5), it is also possible to calculate the space dependence of the electron density [5]:

$$N(z) = \int dv f(z,v) = \frac{4N_0}{v_0}\sum_{n=0}^{\infty}\frac{1}{J_p(j_{p-1,n})} \cdot \exp\left[-\frac{4j_{p-1,n}^2\beta}{v_0^4} z\right]\frac{1}{2} j_{p-1,n}^{p-3/2} \cdot \int_0^{j_{p-1,n}} x^{(1/2)-p} J_p(x)dx. \quad (7)$$

The evolution of the electron distribution function with depth is reported in Fig. 1. The broadening of the spectrum as the electrons enter the target is apparent. Depth and speed are fractions of $4\beta/v_0^4$ and v_0 respectively. To better illustrate the spectrum broadening Fig. 2 shows the electron spectra for different

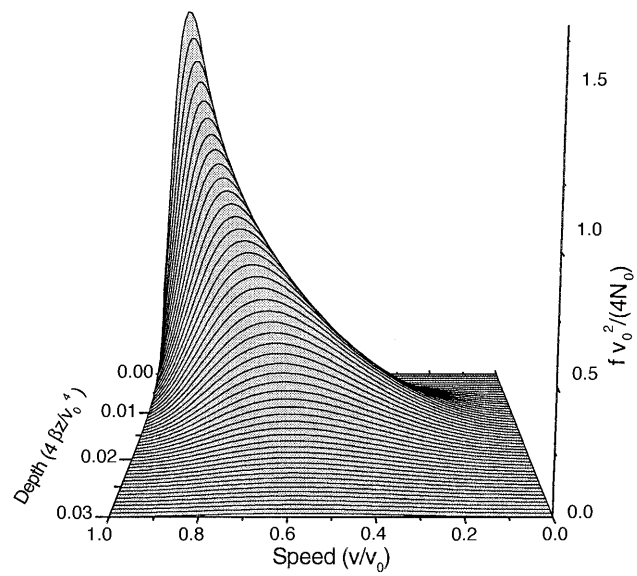

Fig. 1. Electron distribution function (5) as a function of dimensionless energy (speed) and space (depth)

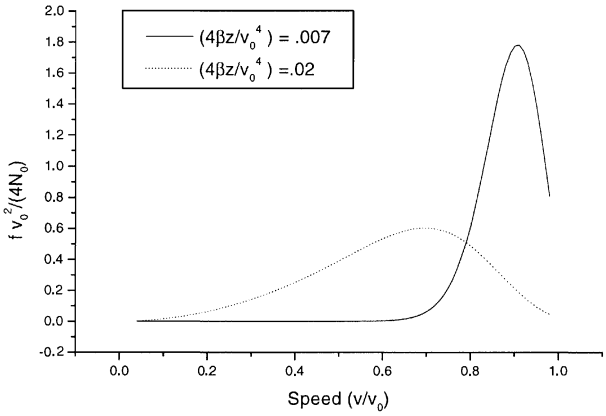

Fig. 2. Dimensionless distribution function of the electrons as a function of dimensionless energy (speed) at different depths, computed with Eq. (5)

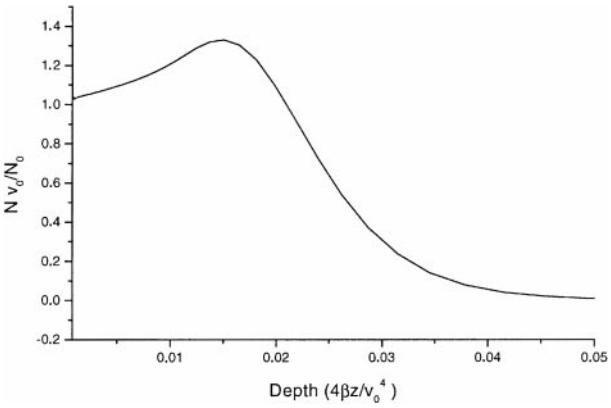

Fig. 3. Electron density number as a function of the depth, computed with Eq. (7)

path lengths. Figure 3 shows the electron density variation law.

So far a plane electron source has been considered. However since the angular straggling has been neglected these results are assumed to be valid also for a narrow electron beam. In this case N must be considered as the electron density averaged over the beam section.

Photon Transport

To predict how the photons, produced by electrons, diffuse through the target the photon transport equation must be considered [6, 7]. The particular geometrical arrangement of the system suggests use of the integral form of the transfer equation

$$\begin{aligned} f(\vec{r},\vec{\omega},\lambda) = \Gamma(\vec{r}_e,\vec{\omega},\lambda)\cdot\exp\left[-\int_0^{|\vec{r}_e-\vec{r}|} ds\mu(\vec{r}-\vec{\omega}s,\lambda)\right] \\ + \int_0^{|\vec{r}_e-\vec{r}|} ds' q(\vec{r}-\vec{\omega}s',\vec{\omega},\lambda) \\ \cdot\exp\left[-\int_0^{s'} ds''\mu(\vec{r}-\vec{\omega}s'',\lambda)\right] \\ + \int_0^{|\vec{r}_e-\vec{r}|} ds' K(\vec{r}-\vec{\omega}s',\vec{\omega}\cdot\vec{\omega}',\lambda'\to\lambda) \\ \cdot f(\vec{r}-\vec{\omega}s',\vec{\omega}',\lambda') \\ \cdot\exp\left[-\int_0^{s'} ds''\mu(\vec{r}-\vec{\omega}s'',\lambda)\right] \end{aligned} \tag{8}$$

Γ is the incoming angular flux at the bounding surface, q is an external source and k is the interaction kernel describing the effects of the interactions of photons with matter.

Instead of the actual source distribution, as obtained by using Eqs. (5) and (7), let us consider a point isotropic and monochromatic source within the slab.

Adopting a cylindrical coordinate system (ρ, z, Φ) with z-axis normal to the target surface and with the point source on it at depth $z = z_0$, Eq. (8) becomes

$$\begin{aligned} f(\rho,z,\cos\vartheta,\varphi,\lambda) = \left\{U(\cos\vartheta)\int_0^{(z/\cos\vartheta)} ds + U(-\cos\vartheta)\int_0^{(z-a)/\cos\vartheta} ds\right\}\cdot\int_0^{\infty} d\lambda'\int_{4\pi} d\vec{\omega}' \\ \cdot k\left(\cos\vartheta\cos\vartheta' + \frac{\rho\cos(\varphi-\varphi') - s\sin\vartheta\cos\varphi'}{\sqrt{\rho^2+s^2\sin^2\vartheta-2\rho s\sin\vartheta\cos\varphi}}\sin\vartheta\sin\vartheta',\lambda'\to\lambda\right) \\ \cdot f\left(\sqrt{\rho^2+s^2\sin^2\vartheta-2\rho s\sin\vartheta\cos\varphi}, z-s\cos\vartheta,\cos\vartheta',\varphi',\lambda'\right)\exp[-\mu(\lambda)s] \\ + \frac{S_0}{8\pi^2}\delta(\lambda-\lambda_0)\left\{U(\cos\vartheta)\int_0^{(z/\cos\vartheta)} ds + U(-\cos\vartheta)\int_0^{(z-a)/\cos\vartheta} ds\right\} \\ \cdot\frac{\delta\left(\sqrt{\rho^2+s^2\sin^2\vartheta-2\rho s\sin\vartheta\cos\varphi}\right)}{r}\delta(z-z_0-s\cos\vartheta)\exp[-\mu(\lambda)s] \end{aligned} \tag{9}$$

where a is the thickness of the slab. The kernel is composed of three terms corresponding to Compton scattering, Rayleigh scattering and photoelectric effect, which are the most important processes in the X-ray regime. In this paper we are mainly interested in photoelectric effect so the kernel will be simply [8–10]

$$k\left(\cos\vartheta\cos\vartheta'+\frac{\rho\cos(\varphi-\varphi')-s\sin\vartheta\cos\varphi'}{\sqrt{\rho^2+s^2\sin^2\vartheta-2\rho s\sin\vartheta\cos\varphi}}\cdot\sin\vartheta\sin\vartheta',\lambda'\to\lambda\right)=\frac{1}{4\pi}\sum_i Q_{\lambda_{e_i}}(\lambda')\delta(\lambda-\lambda_i)U(\lambda_{e_i}-\lambda') \tag{10}$$

$Q_{\lambda i}$ is the emission probability for the i-th line which is emitted only when λ' is lower that the absorption edge wavelength λ_{ei}. The lines are assumed monochromatic, neglecting their natural width. In the computation of attenuation coefficient all the processes are considered.

The solution can be approached by constructing a Neumann type series of the powers of the equation kernel. This means that the angular flux is expressed as the sum of the angular fluxes of the unscattered photons, of the once scattered photons and so on. Since the complexity of the calculations rapidly increases with the number of the iterations, it will be possible to compute analytically only the first terms of this series. However few terms are sufficient to give useful information on the radiation field.

The flux of the unscattered photons is found simply neglecting the in-scattering term in (9)

$$f_0(\rho,z,\cos\vartheta,\varphi,\lambda)=\frac{S_0}{4\pi}\delta(\varphi)\delta(\lambda-\lambda_0)\cdot\frac{1}{\rho\sin\vartheta|\cos\vartheta|}\delta\left(\frac{\rho}{\sin\vartheta}-\frac{z-z_0}{\cos\vartheta}\right)\cdot\exp\left[-\mu(\lambda_0)\frac{\rho}{\sin\vartheta}\right] \tag{11}$$

The flux of the primary photons produced by photoelectric effect is calculated by neglecting the external source and by substituting f with f_0 in the in-scattering term obtaining Eqn. (12).

The solution can be used as Green function to determine the primary photon radiation field, when the source distribution is known.

If a narrow electron beam enters the target, each elementary length dz of the beam path can be considered as an isotropic point source whose intensity is estimated in electron per unit time by

$$\sum_i S_i(\vec{r})=N(z)\sum_i P_i(z)dz \tag{13}$$

where N is given by (7). P_i is the emission probability of the i-th line, which depends on the ionization cross sections and, consequently, on the energy spectrum of the electrons.

Let us assume that all the ionization processes take place on the axis of the beam, so that the flux of the source photons is given by

$$\begin{aligned}f_0(\rho,z,\cos\vartheta,\varphi,\lambda)&=\sum_i\frac{1}{4\pi}\delta(\varphi)\delta(\lambda-\lambda_i)\int_0^a dz_0\frac{S_i(z_0)}{\rho\sin\vartheta|\cos\vartheta|}\cdot\delta\left(\frac{\rho}{\sin\vartheta}-\frac{z-z_0}{\cos\vartheta}\right)\exp\left[-\mu(\lambda)\frac{\rho}{\sin\vartheta}\right]\\&=\sum_i\frac{1}{4\pi}\delta(\varphi)\delta(\lambda-\lambda_i)\frac{S_i(z-\rho\cot\vartheta)}{\rho\sin\vartheta}\cdot U(z-\rho\cot\vartheta)U(a-z+\rho\cot\vartheta)\cdot\exp\left[-\mu(\lambda)\frac{\rho}{\sin\vartheta}\right]\end{aligned} \tag{14}$$

The angular flux of the primary photons is given by Eqn. (15).

The description of the radiation field of unscattered and primary photons is complete and pointwise. The result is useful not only for numerical computation but also for a better insight into the photon diffusion and a better interpretation of experimental result.

$$f_1(\rho,z,\cos\vartheta,\varphi,\lambda)=\frac{S_0}{4\pi}\sum_i U(\lambda_{e_i}-\lambda_0)\delta(\lambda-\lambda_i)\frac{Q_{\lambda_i}(\lambda_0)}{4\pi}\left\{U(\cos\vartheta)\int_0^{(z/\cos\vartheta)}ds+U(-\cos\vartheta)\int_0^{(z-a)/\cos\vartheta}ds\right\}\cdot\frac{1}{[s-\rho\sin\vartheta\cos\vartheta-(z-z_0)\cos\vartheta]^2-(\rho\sin\vartheta\cos\vartheta+(z-z_0)\cos\vartheta)^2+r^2+(z-z_0)^2}\cdot\exp\left[-\mu(\lambda_0)\sqrt{\cdot[s-\rho\sin\vartheta\cos\vartheta-(z-z_0)\cos\vartheta]^2-(\rho\sin\vartheta\cos\vartheta+(z-z_0)\cos\vartheta)^2+r^2+(z-z_0)^2}-\mu(\lambda)s\right] \tag{12}$$

$$f_1(\rho,z,\cos\vartheta,\varphi,\lambda)=\sum_i\sum_j\frac{1}{4\pi}U(\lambda_{e_i}-\lambda_j)\delta(\lambda-\lambda_i)\frac{Q_{\lambda_i}(\lambda_j)}{4\pi}\left\{U(\cos\vartheta)\int_0^{(z/\cos\vartheta)}ds+U(-\cos\vartheta)\int_0^{(z-a)/\cos\vartheta}ds\right\}\cdot\int_0^a dz_0$$
$$\cdot\frac{S_j(z_0)}{[s-\rho\sin\vartheta\cos\vartheta-(z-z_0)\cos\vartheta]^2-(\rho\sin\vartheta\cos\vartheta+(z-z_0)\cos\vartheta)^2+r^2+(z-z_0)^2}$$
$$\cdot\exp\left[-\mu(\lambda_j)\sqrt{\cdot[s-\rho\sin\vartheta\cos\vartheta-(z-z_0)\cos\vartheta]^2-(\rho\sin\vartheta\cos\vartheta+(z-z_0)\cos\vartheta)^2+r^2+(z-z_0)^2}-\mu(\lambda)s\right] \tag{15}$$

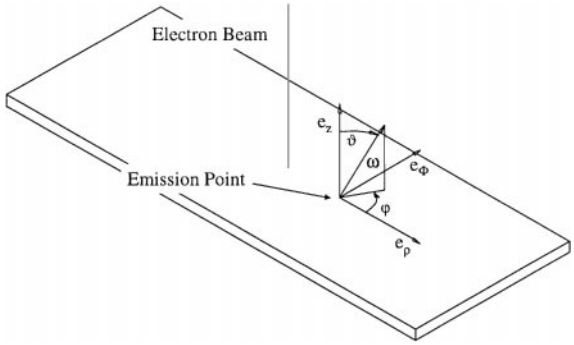

Fig. 4. System geometry

As an example we have considered a binary target composed of a mixture of 50% Al and 50% Si. In order to show the descriptive power of the solution, in Fig. 5a – 5d we have reported the 3D polar plots of the angular distributions of the primary photoelectric photons, coming out of the slab from a well defined point of the surface. These photons are emitted by aluminum atoms excited by silicon photons. To interpret the plots one must refer to the scheme reported in Fig. 4, that explains the geometry of the problem. In the polar plots the quantity $\int_{4\pi}d\vec{\omega}f(\vec{r},\vec{\omega},\lambda)/(\Delta\vartheta)(\Delta\varphi)$ has been reported with $\Delta\vartheta=\pi/100$ and $\Delta\varphi=2\pi/100$. The isotropy of the

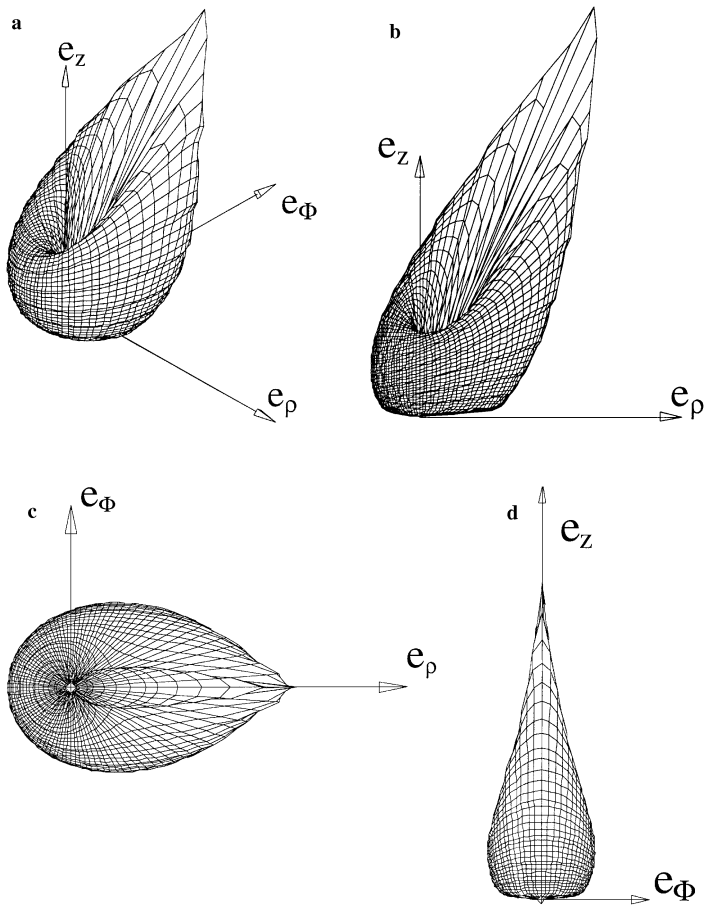

Fig. 5. Angular distribution of the primary photoelectric photons at an emission point placed on the slab surface. (a) 3D view; (b) Side view; (c) Top view; (d) Front view

photoelectric emission determines a full angular spread of primary photons.

Conclusions

In this work electron slowing down has been studied with the Fokker-Planck equation for a stationary and monodimensional source. Directional straggling has been neglected with respect to the much more important energy dispersion. Energy and space electron distribution function has been computed analytically, by solving the equation. This is an important progress in comparison with the continuous slowing down approximation, where all the electrons are supposed to have the same energy. The depth distribution of the primary photon sources has been then evaluated by averaging on energy the ionization cross sections.

The distribution in physical and momentum space of the source photons produced has been also determined, by using the integral form of the transport equation. Then the first order correction due to the prevailing photoelectric effect has been described. The effects of the geometry of the system and of the boundary conditions have been fully considered.

The results have been presented in as general a form as possible. It is worth noting that the two equations of transfer have been solved separately. It is foreseen a further development by considering higher order terms of the series for the solution and a comparison with the ZAF approach.

References

[1] L. V. Spencer, *Phys. Rev.* **1955**, *98*, 1597.
[2] H. W. Lewis, *Phys. Rev.* **1950**, *78*, 526.
[3] S. Woolf, W. L. Filippone, B. D. Ganapol, J. C. Garth, *Nucl. Sci. Eng*. **1986**, *92*, 110.
[4] W. L. Filippone, *Nucl. Sci. Eng*. **1986**, *92*, 421.
[5] S. Manservisi, V. Molinari, A. Nespoli, *Nuovo Cimento D* **1995**, *18*, 4.
[6] U. Fano, L. V. Spencer, M. J. Berger, '*Handbuch der Physik* XXXVIII/2. In: S. Flugge (Ed.) Springer, Berlin Heidelberg New York Tokyo 1960, pp. 660 – 817.
[7] G. C. Pomraning, *The Equations of Radiation Hydrodynamics*. Pergamon Press, Oxford, 1973.
[8] J. E. Fernández, *X-ray Spectrom*. **1989**, *18*, 271.
[9] W. H. Mc Master, N. Kerr del Grande, J. H. Mallett, J. H. Hubbell, *Compilation of X-Ray Cross-Sections*, Lawrence Livermore National Laboratory Report UCRL-50174, Section 2, Rev. 1, 1969.
[10] J. H. Scofield, *Theoretical Photo-Ionization Cross-Sections from 1 to 1500 KeV*, Lawrence Livermore National Laboratory Report UCRL-51326, 1973.
[11] J. E. Fernández, V. G. Molinari, *Advances in Nuclear Science and Technology 22*. In: J. Lewins, M. Becker (Eds.) Plenum Press, New York, 1991, pp. 45 – 104.